contributions

Wide-Angle Microwave Lens for Line Source Applications*

W. ROTMAN†, MEMBER, IEEE, AND R. F. TURNER‡

Summary—A new "time-delay" scanner consists of a constrained wide-angle two-dimensional microwave lens with a straight front face in which lens elements connect arbitrary points on the inner and outer contours. The lens can operate at very short pulse lengths and can scan more beamwidths than any previously known device of its type. A phase analysis shows that this design has very small coma aberrations and that the lens can generate fractional degree beams. Criteria developed for selecting optimum lens parameters are given.

The radiation patterns of an experimental model in which the lens elements consist of coaxial cables show the expected wide-angle characteristics. In further tests incremental scanning was obtained through the use of phase shifters in the coaxial lens elements. The design of symmetrical three-dimensional lenses is briefly discussed. A table of lens contour parameters is given for an optimum lens design with scan angle α of 30°.

INTRODUCTION

THE WIDE-ANGLE scanning characteristics of two-dimensional microwave lenses have been extensively studied[1] for radar antenna applications. Ruze[2] has shown, for example, that constrained lenses are capable of scanning one-degree beams over angles as great as 100 beamwidths. His lens design has two perfect off-axis symmetrical focal points and an on-axis focal point for which the second-, but not higher-order phase deviation is zero. For these no-second-order lenses both front and back lens contours are curved.

Ruze also discusses the design of a lens with a straight front face for use as the primary illuminator for a parabolic cylindrical reflector or for a planar array. This straight-front-face lens has excellent scanning characteristics since both second- and third-order coma aberrations may be almost eliminated by proper refocusing. It has two perfect symmetrical off-axis and one highly corrected on-axis focal points. For very narrow beam antennas, however, its higher-order coma aberrations may be objectionable.

It is the purpose of this paper to show how these coma aberrations in the straight-front-face lens may be still further reduced by the use of general lens design principles developed by Gent, *et al.*[3,4] This new design gives a lens with three perfect focal points of which one is on the central axis and the other two are symmetrically located on either side. The design equations for this lens are derived and its phase aberrations and scanning capabilities are evaluated. Experimental results on a test model are also presented.

* Received August 31, 1962; revised manuscript received May 17, 1963.

† Air Force Cambridge Research Labs., L. G. Hanscom Field, Bedford, Mass.

‡ Electronic System Division, L. G. Hanscom Field, Bedford, Mass.

[1] J. Brown, "Microwave Lenses," Methuen and Co., Ltd., London, England, ch. vi, pp. 69–82; 1953.

[2] J. Ruze, "Wide-angle metal-plate optics," PROC. IRE, vol. 38, pp. 53–58; January, 1950.

[3] S. S. D. Jones, H. Gent, and A. A. L. Browne, "Improvements in or Relating to Electromagnetic-Wave Lens and Mirror Systems," British Provisional Patent Specification No. 25926/56; August, 1956.

[4] H. Gent, "The Bootlace Aerial," *Roy. Radar Establishment J.*, pp. 47–57; October, 1957.

Derivation of Lens Parameters

This new lens design (which will be labeled as the Gent model) differs from the Ruze model in that corresponding points on the two lens contours (the Y and N parameters in Fig. 1) are not equidistant from the central axis. This change can be made readily in experimental models by using flexible coaxial cables, rather than waveguide, as lens elements. The additional degree of freedom in design permits the specification of four independent conditions which determine the lens parameters uniquely, rather than the three conditions that were available to Ruze. In the present lens design, these four parameters are selected as the straight front face, two symmetrical off-axis focal points and an on-axis focal point. A schematic representation of a parallel plate microwave lens of this type in which the coaxial microwave lens elements are connected directly to a straight line of radiators to form a line source is shown in Fig. 2.

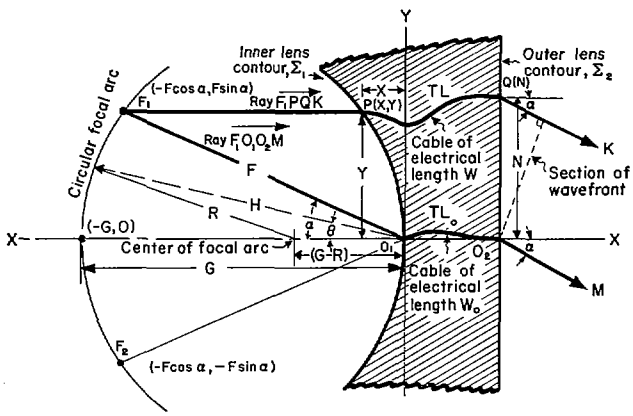

Fig. 1—Microwave lens parameters.

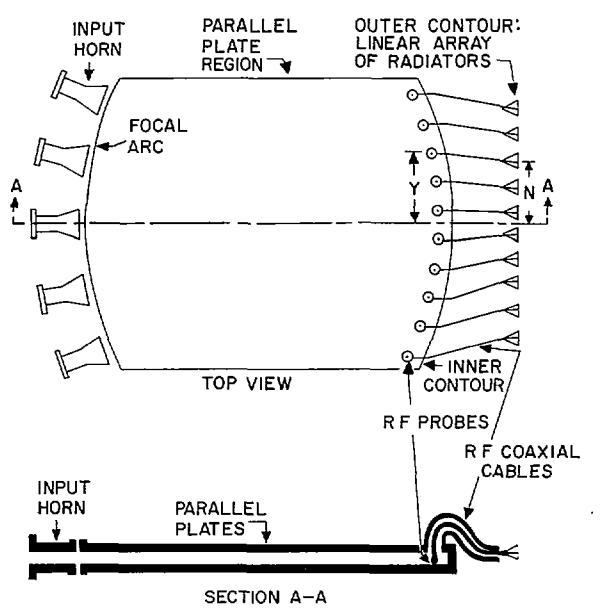

Fig. 2—Parallel-plate microwave lens.

This lens design uses the generalized equations obtained by Gent[3] for lenses of arbitrary shape. In Fig. 1, the lens contours are shown by the curves Σ_1 and Σ_2. The inner contour Σ_1 is determined by the design equations and locates the position of the probe transitions (Fig. 2) between the parallel plates and the coaxial cables. The outer contour Σ_2 is straight and defines the position of the radiating elements that comprise the line source. Corresponding elements on contours Σ_1 and Σ_2 are connected by coaxial transmission lines.

The contour Σ_1 is defined by the two coordinates (X, Y) that are specified relative to a point O_1 on the central axis of the lens. Elements on the straight contour Σ_2 are similarly determined by the single coordinate N, measured relative to the point O_2. O_1 and O_2 lie on contours Σ_1 and Σ_2, respectively, and are connected by a transmission line TL_0 of electrical length W_0. The point $P(X, Y)$ is a typical element in Σ_1 and is connected to element $Q(N)$ which lies on Σ_2 by the transmission line TL of electrical length W. Since the three parameters X, Y and W are independent, the straight-front-face lens has three degrees of freedom to be stipulated. (Other types of lenses, including the Ruze model for which $Y=N$, have at least one less degree of freedom.) These three degrees of freedom are now used to obtain wide-angle scanning characteristics by selecting (Fig. 1) two symmetrical off-axis focal points F_1 and F_2, and one on-axis focal point G, having coordinates $(-F\cos\alpha, F\sin\alpha)$, $(-F\cos\alpha, -F\sin\alpha)$ and $(-G, O)$, respectively, relative to the point O_1. A central ray which passes through the origin of the lens is represented by $\overrightarrow{F_1O_1O_2M}$; $\overrightarrow{F_1PQK}$ represents any other ray which originates from the point F_1. F_1, F_2 and G are points of perfect focus for radiation at angles to the axis of $-\alpha$, $+\alpha$ and 0°, respectively.

Gent's equations for optical path-length equality between a general ray and the ray through the origin become for our case

$$\overrightarrow{(F_1P)} + W + N\sin\alpha = F + W_0, \tag{1}$$

$$\overrightarrow{(F_2P)} + W - N\sin\alpha = F + W_0 \tag{2}$$

and

$$\overrightarrow{(G_1P)} + W = G + W_0 \tag{3}$$

where

$$\overrightarrow{(F_1P)} = F^2 + X^2 + Y^2 + 2FX\cos\alpha - 2FY\sin\alpha, \tag{4}$$

$$\overrightarrow{(F_2P)} = F^2 + X^2 + Y^2 + 2FX\cos\alpha + 2FY\sin\alpha \tag{5}$$

and

$$\overrightarrow{(GP)}^2 = (G + X)^2 + Y^2. \tag{6}$$

(These equations may also be derived directly from the geometry of Fig. 1.) $\overrightarrow{F_1P}$, $\overrightarrow{F_2P}$ and $\overrightarrow{GP}$ are the path lengths from focal points F_1, F_2 and G, respectively, to the point P on the inner lens contour.

A set of parameters which are normalized relative to the focal length F is now defined,

$$\eta = N/F, \qquad x = X/F, \qquad y = Y/F,$$

$$w = \frac{W - W_0}{F}, \qquad g = G/F.$$

Also,

$$a_0 = \cos \alpha, \qquad b_0 = \sin \alpha.$$

Eqs. (4) to (6) become

$$\frac{(\overrightarrow{F_1P})^2}{F^2} = 1 + x^2 + y^2 + 2a_0x - 2b_0y, \tag{4a}$$

$$\frac{(\overrightarrow{F_2P})^2}{F^2} = 1 + x^2 + y^2 + 2a_0x + 2b_0y \tag{5a}$$

and

$$\frac{(\overrightarrow{GP})^2}{F^2} = (g + x)^2 + y^2. \tag{6a}$$

The normalized forms of (1) and (4) are now combined.

$$\begin{aligned}\frac{(\overrightarrow{F_1P})^2}{F^2} &= (1 - w - b_0\eta)^2 \\ &= 1 + w^2 + b_0^2\eta^2 - 2b_0\eta + 2b_0w\eta - 2w \\ &= 1 + x^2 + y^2 + 2a_0x - 2b_0y. \end{aligned} \tag{7}$$

Since the off-axis focal points are located symmetrically about the center axis, the lens contours must also be symmetrical. Therefore, (7) remains unchanged and can be separated into two independent equations if η is replaced by $-\eta$ and y by $-y$. One equation contains only odd powers of y and η while the other contains the even terms. Thus,

$$-2b_0\eta + 2b_0w\eta = -2b_0y \tag{8}$$

or

$$y = \eta(1 - w).$$

Also,

$$x^2 + y^2 + 2a_0x = w^2 + b_0^2\eta^2 - 2w. \tag{9}$$

Eqs. (3) and (6), relating to the on-axis focus, are likewise combined.

$$\frac{(\overrightarrow{GP})^2}{F^2} = (g - w)^2 = (g + x)^2 + y^2 \tag{10}$$

or

$$x^2 + y^2 + 2gx = w^2 - 2gw. \tag{11}$$

After algebraic manipulation, (9) and (11) give the following relation between w and η:

$$aw^2 + bw + c = 0 \tag{12}$$

where

$$a = \left[1 - \eta^2 - \left(\frac{g - 1}{g - a_0}\right)^2\right],$$

$$b = \left[2g\left(\frac{g - 1}{g - a_0}\right) - \frac{(g - 1)}{(g - a_0)^2}b_0^2\eta^2 + 2\eta^2\right] - 2g$$

and

$$c = \left[\frac{gb_0^2\eta^2}{g - a_0} - \frac{b_0^4\eta^4}{4(g - a_0)^2} - \eta^2\right].$$

For fixed values of design parameters α and g, w can be computed as a function of η from (12). These values of w and η are substituted into (8) and (11) to determine x and y, completing the solution for the lens design.

This procedure gives a lens which has three perfect focal points corresponding to the angles $\pm\alpha$ and 0°. For wide-angle scanning the lens must focus well, not only at these three points, but also at all intermediate angles along the focal arc. The basic lens equations, however, do not specify the optimum value of the factor g (ratio of on-axis to off-axis focal length G/F) which minimizes the over-all phase aberrations.

This optimum value may be obtained by analog to the phase error analysis[2] of the Ruze lens for which $y=\eta$. His lens design has two perfect focal points F_1 and F_2 which are located on a circular focal arc with its center at the origin of the contour Σ_1. For his straight-front-face lens, Ruze shows that the optical aberrations are minimized by refocusing the feed radically from this focal arc by an amount equal to $\frac{1}{2}(\alpha^2-\theta^2)F$ where θ is an angle (Fig. 1) at which correction is required. The residual aberrations are then small and the lens can scan a narrow beam over wide angles, using the new focal arc which passes through both these refocused points and the points of perfect focus. The Gent ($y\neq\eta$) and Ruze ($y=\eta$) designs for a straight-front-face lens are almost similar when the optimum focal arc is selected as outlined above since the on-axis aberrations for the Gent design are zero while in the latter case these aberrations are minimized. A value of g which gives the same on-axis focal position for both types of lenses was therefore selected as a reasonable estimate for an optimum design, corresponding to the refocused value for $\theta=0°$,

$$g = \frac{G}{F} = 1 + \frac{\alpha^2}{2}. \tag{13}$$

The focal arc is now selected (Fig. 1) as a portion of a circle of radius R, which passes through the two symmetrical off-axis and one on-axis focal points. The optical aberrations of the lens are defined as the difference in path lengths between a central ray through

the origin and any other ray, both of which are traced from an arbitrary point on the focal arc through the lens and terminate normal to the emitted wavefront. This path length error is a function both of the scan angle θ and the position along the lens contour η, and may be derived geometrically [in a manner similar to that of (1) through (6)] from Fig. 1 as

$$\Delta l = \frac{L\Delta}{F} = (h^2 + x^2 + y^2 + 2hx\cos\theta - 2hy\sin\theta)^{1/2} - h + w + \eta\sin\theta \tag{14}$$

where ΔL is the path length error and $h\ (=H/F)$ is the normalized distance from a point on the focal arc to the origin O_1 of surface Σ_1. H is computed by the law of cosines from the triangle with sides R, H and $(G-R)$ and included angle θ (Fig. 1); θ is the angle between central axis and an arbitrary point on the focal arc, and R is the radius of the focal arc which is determined by the three points G, F_1 and F_2.

Our selected value of the lens parameter g was chosen for minimum optical aberrations over a prescribed range of scan angles. This design procedure assumes that the correction for second- and third-order coma terms also results in the minimization of the higher-order aberrations. Since this assumption has not been proven analytically, path-length errors were computed numerically for a typical lens design to determine whether (13) gives an optimum estimate of the g factor. For a selected half scan angle α of 30°, the corresponding value of g is equal to 1.137. The normalized lens contour parameters y, x and w and the path-length error Δl were therefore computed from (8), (11), (12) and (14) for the following range of parameters which are centered about the optimum g value:

$$g = 0.90\langle 0.05\rangle 1.20, \quad \text{and} \quad 1.137;$$
$$\theta = \pm 5°, \pm 15°, \pm 25°, \pm 35° \quad \text{and} \quad \pm 40°;$$
$$\eta = 0\langle 0.05\rangle 0.80;$$
$$\alpha = 30°.$$

For $\theta = 0°$ and $\pm 30°$, Δl is identically zero. Tables of these lens parameters are given in Rotman and Turner.[5] Selected lens contour curves are shown in Figs. 3(a) to 3(d) for g equal to 1.00, 1.10, 1.137 and 1.20; a short table of contour values is given in the Appendix for g equal to 1.137. The light lines between the inner and outer contours indicate corresponding values of y and η which are the junction points for the transmission line elements.

A comparison is made in Fig. 3(c) between the inner lens contour for the Gent and the Ruze designs for the optimized value of $g = 1.137$. In the latter case, the design equations for the straight-front-face lens are

$$x^2 + a_0^2 y^2 + 2a_0 x = 0,$$
$$w = 0, \quad \text{and} \quad \eta = y. \tag{15}$$

This elliptical inner contour does not depend upon the value of g. The contours for both $y \neq \eta$ and $y = \eta$ lenses almost coincide for values of η less than 0.65 in agreement with our original assumption.

The contour for which $g = 1.00$ [Fig. 3(b)] is also of interest in that it is the only case for which the focal arc is centered at the vertex O_1 of the inner lens face and for which the central ray paths from all points on the focal arc are equal in length. Such considerations may be of importance in monopulse applications. This lens contour has been discussed by Hatcher[6] who showed that its shape could be approximated by a segment of a circle. Its optical abberations are considerably poorer than those for the optimum design, however,

Optical aberrations, expressed as the normalized path length errors Δl, are given in Fig. 4 for selected values of g equal to 1.00, 1.10 and 1.137. For values of η less than ± 0.53, (13) predicts the optimum value of g (1.137) in the sense that the path-length error Δl remains a minimum (below ± 0.0001) for all angles of scan up to $\pm 35°$. If the permissible path-length error Δl can be as great as ± 0.0005, however, a lens design with g equal to 1.10 may be more suitable since it would permit the use of larger apertures (up to $\eta = 0.8$). Note that the path-length errors for the lens design with g equal to 1.00 have essentially even symmetry with respect to η while those for g equal to 1.10 and 1.137 have odd symmetry.[7]

The path-length errors as well as the operating wavelength and size of the antenna aperture determine the minimum beamwidth obtainable from a microwave lens. The half-power beamwidth (HPBW) for a rectangular aperture antenna with a cosine illumination taper (which has maximum sidelobes of 23 db) is given by

$$\text{HPBW} = 69° \times \frac{\lambda}{D} \tag{16}$$

where

$D\ (=2N_{\max}\cos\theta)$ is the project aperture,

$N_{\max}$ is one half of the physical aperture

and

λ is the wavelength.

The maximum path-length error deviation $(2\Delta L_{\max})$ cannot exceed about $\lambda/4$ without affecting the sidelobe level adversely. Thus,

$$(\Delta L)_{\max} = \frac{\lambda}{8}. \tag{17}$$

[5] W. Rotman and R. F. Turner, "Wide-angle microwave lens for line source applications," AF Cambridge Research Labs., Bedford, Mass., Tech. Rept. No. AFCRL 62-18; January, 1962.

[6] B. R. Hatcher, "Multiple-beam interval scanning antenna feasibility and development study," Chu Associates, Littleton, Mass., Final Engrg. Rept. No. AFCRC-TR-60-146, Contract No. AF19(604)-5202; May, 1960.

[7] The curves of path-length error show only positive values for θ while η assumes both positive and negative values. Alternatively, both positive and negative values of θ could be used with positive values of η.

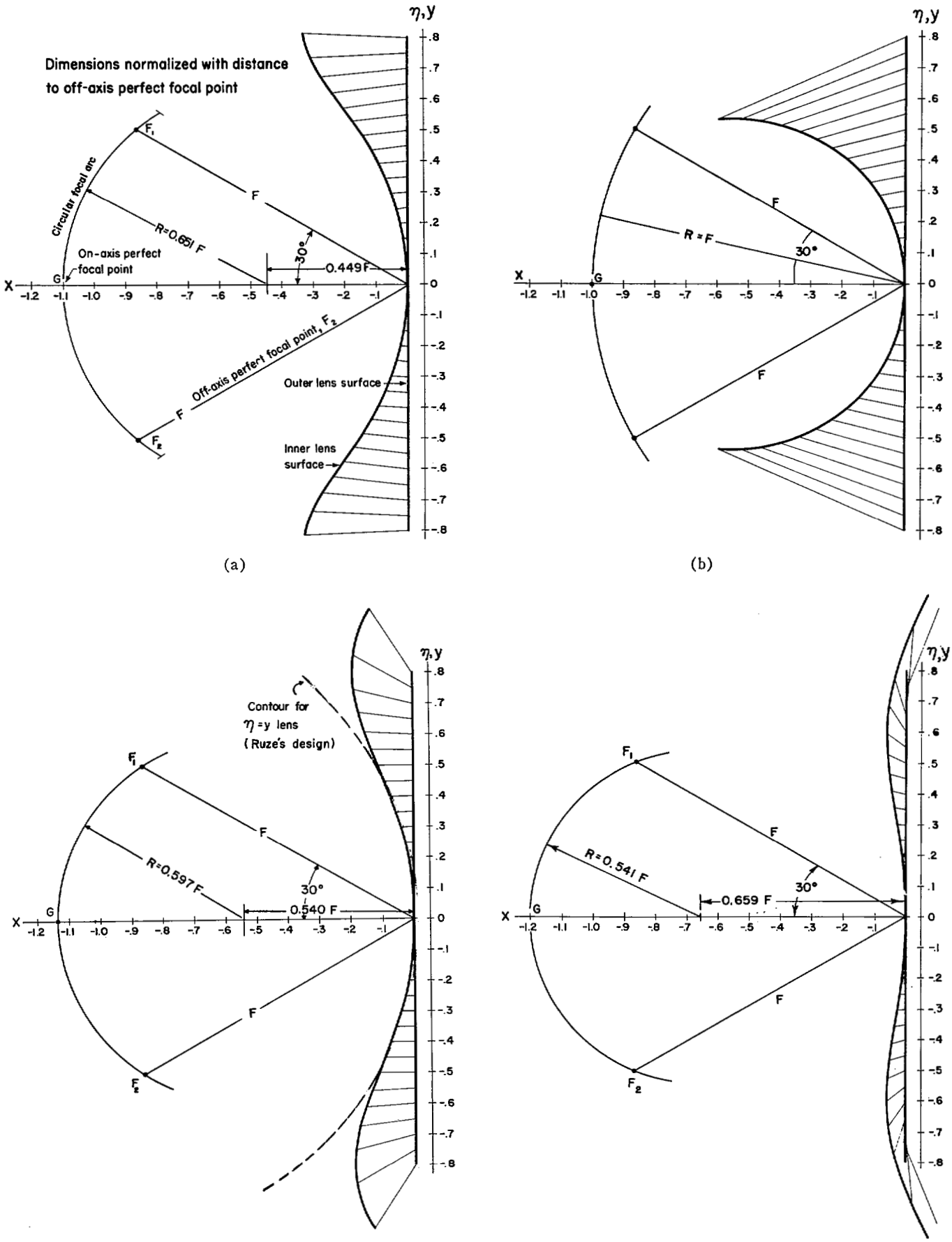

Fig. 3—Microwave lens contours. (a) $g=1.10$. (b) $g=1$. (c) $g=1.137$. (d) $g=1.20$.

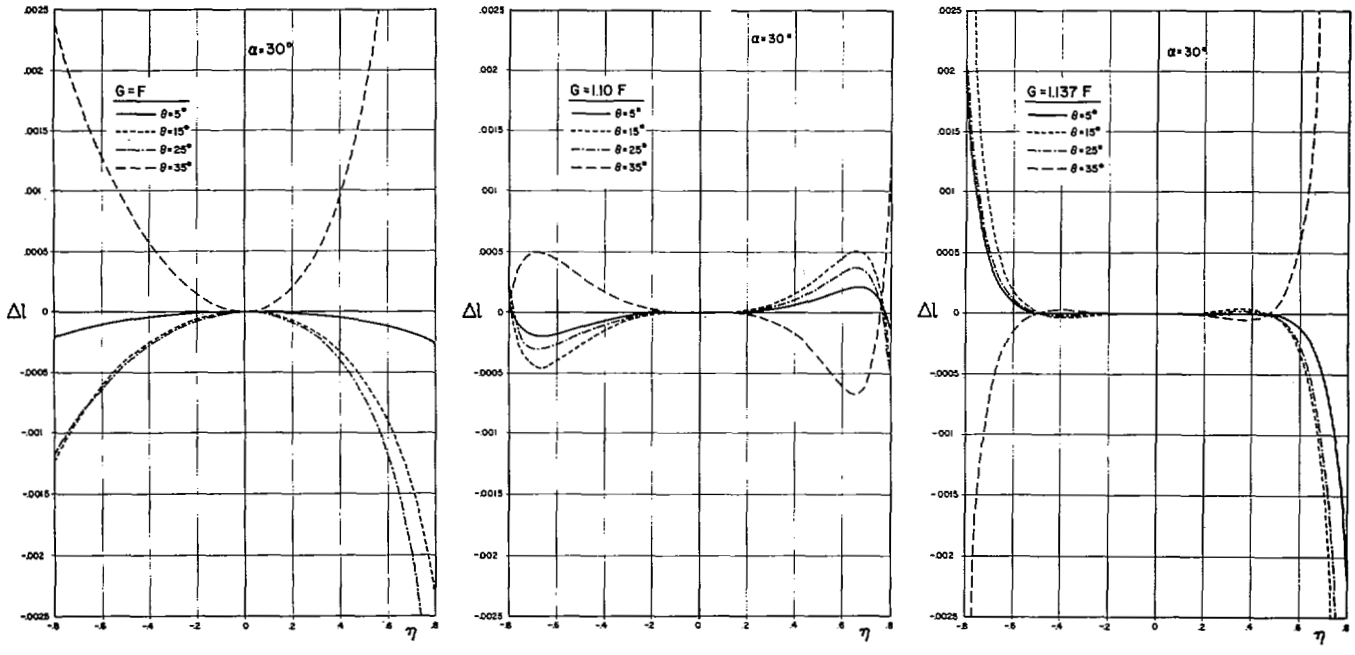

(a) (b) (c)

Fig. 4—Path-length errors in microwave lens. (a) $g=1.00$. (b) $g=1.10$. (c) $g=1.137$.

Eqs. (16) and (17) are combined and normalized to give

$$\frac{D}{\lambda}=\frac{\eta_{\max}\cos\theta}{2(\Delta l)_{\max}} \tag{18}$$

and

$$(\mathrm{HPBW})_{\min}=\frac{(\Delta l)_{\max}}{\eta_{\max}\cos\theta}\times 276^\circ \tag{19}$$

where $(\mathrm{HPBW})_{\min}$ is the minimum possible beamwidth for a given lens aperture.

The wide-angle characteristics of a lens design is expressed in the number of beamwidths that can be scanned. The following lens parameters are chosen for illustrative purposes: $\alpha=30°$, $g=1.137$, $\eta_{\max}=0.55$, $G/D=g/2\eta_{\max}=1.035$ and $(\Delta l)_{\max}=0.00013$ (from Fig. 4). Then $(\mathrm{HPBW})_{\min}=0.075°$ for $\theta=30°$. A beam of less than 0.1°, therefore, can be scanned over an angle of 60° (2α). This is a scan capability of 800 beamwidths. In this example the scan angle θ can be extended to $\pm 35°$ with little additional path-length errors. Note that refocusing from a circular focal arc to some other noncircular arc that also passes through F_1, F_2 and G does not reduce coma aberrations substantially since refocusing affects primarily the symmetrical path-length errors whereas the residual aberrations (except for the case where g equals unity) are primarily asymmetrical.

The lens contour for which g equals 1.137 is thus optimized in that this minimizes the obtainable beamwidth for moderate ratios of focal length to lens aperture (F/D ratio). For cases in which even smaller ratios of F/D are required and where the phase error tolerance can be relaxed, smaller values of g (such as 1.10) may be more suitable.

Experimental Results

A wide-angle microwave lens model based upon the derived design equations was constructed for test purposes. Design specifications include the following parameters: $f_0=3.0$ Gc, $g=1.137$, $\eta_{\max}=0.60$, $D/\lambda=18$, $\theta_{\max}=30°$, HPBW = 3°. A sketch of the microwave lens model is shown in Fig. 5. The lens elements are RG-9/U coaxial cables and the primary illuminator is an open-ended waveguide horn. The lens contour and phase errors of this model are shown in Figs. 3(c) and 4(c), respectively.

The theoretical phase errors inherent in this model, whose size and beamwidth are dictated by constructional expediency, are so small that they cannot be detected by their effect on the radiation pattern or other electrical characteristics of the lens. For example, either the Ruze or the Gent designs for g equal to 1.00, 1.10 or 1.137 result in lenses with equivalent electrical performance when the beamwidth is on the order of 3°. The experimental objective is not to evaluate competitive lens designs, but rather to demonstrate techniques unique to the construction of microwave lenses which have variably spaced coaxial lens elements.

The microwave lens model has an inherently large bandwidth since the design is based upon the TEM parallel plate and coaxial modes of propagation for which the phase velocity is frequency-insensitive. In this sense it is a "time-delay" scanner. Its design will now be described for use as a transmitting antenna.

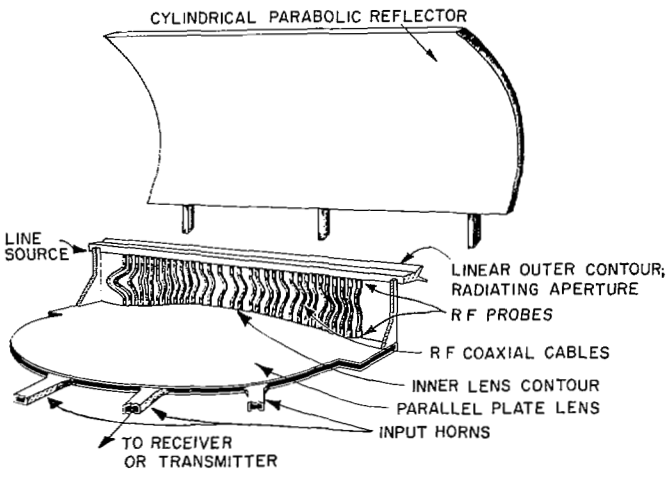

Fig. 5—Parallel-plate lens and reflector.

Microwave radiation from any one of the several input horns, which are located along the focal arc, propagates between the parallel plates in the TEM mode, and illuminates the reflector-backed probes along the inner lens contour which transfer the energy into the coaxial cables and, hence, to a second set of probes on the front lens contour. These probes, in turn, act as a linear array of monopoles that radiate into space through a short, elongated TEM horn transition. The radiating aperture is located along the focal line of a cylindrical parabolic reflector which collimates the beam in the elevation plane. The reflector was not used in the experimental tests for which only azimuthal radiation patterns are of interest.

The design of the input horns is determined by the required amplitude distribution along the front contour of the lens. The required radiation pattern of the horn alone is obtained graphically by ray tracing,[8] equating the power radiated per unit length along the front lens face to that in the angular sector which is subtended from the horn position on the focal arc. The horn aperture and its orientation are then selected[9] to give the closest approximation to the required primary pattern. The ideal lens illumination differs from that physically realizable in that the required primary pattern is not symmetrical (except for the on-axis position $\theta=0°$) and does not conform exactly to that obtainable from a uniformly phased horn. The far-field radiation pattern is, however, not very sensitive to small errors in illumination taper. Since the required directivity of the input horn is a function of its position along the focal arc, its dimensions and orientation likewise depend upon its location. For example, the horn apertures in the present model vary from 1.2λ for the on-axis focal point to 1.45λ for the focal point at $\theta=30°$. Since several stationary horns are used, this variation in horn dimensions causes no difficulty. If the beam were scanned by moving a single-input horn along the focal arc, a compromise aperture dimension (*i.e.*, 1.3λ) would be selected.

The dimensions and spacing of the probes are chosen to ensure adequate coupling of the coaxial cables to the parallel plates for waves incident over a wide range of angles. Although analysis of a set of probes which are located along a curved boundary, mutually coupled and excited by a nonplanar wave, is difficult, the approximate behavior can be obtained by considering an infinite linear array of uniformly spaced probes which are phased to radiate a plane wave at an angle γ relative to the normal of the array. Antenna theory shows that the probe spacing d must satisfy the inequality of (19) to avoid secondary maxima,

$$\frac{d}{\lambda} \leq \frac{1}{|\sin\gamma| + 1} . \tag{19}$$

The probe spacing is therefore restricted to less than λ for broadside radiation ($\gamma=0°$) and $\lambda/2$ for endfire radiation ($\gamma=90°$).

The actual probe spacing in the model can be somewhat greater than that indicated by (19) since this expression applies to a set of omnidirectional probes while the reflector-backed probes have a dipole-like element pattern in which radiation is restricted to a range of angles of about $\pm 60°$ from the normal. This directivity, when combined with the limited range of angles over which the lens operates, permits a maximum probe spacing d of 0.65λ along the inner lens contour. A uniform probe spacing of 0.50λ along the outer, straight lens contour results in a nonuniform spacing along the inner contour which satisfies the above restriction.

The probe dimensions were found experimentally by measuring the input impedance of a single probe when all the others in a parallel-plate array were terminated in matched loads. The results of these tests agreed with power reflection measurements for plane waves incident on the probes at angles up to 60°. Probe dimensions include an element spacing of 0.50λ, parallel-plate spacing of 0.375λ, element-reflector spacing of 0.21λ and element length of 0.15λ.

The theoretical lens contours coincide with the reflecting surface behind the probes since the phase center for a probe imaged in a ground plane is located at the surface of the reflector. In the model, several input horns are used simultaneously to give a number of independent beams. The flexibility of the coaxial cable elements permits displacement of the line source, which forms the straight front face of the lens, from the rest of the structure (Fig. 5).

[8] W. Rotman, "A study of microwave double-layer pillboxes: Part I, line source radiators," AF Cambridge Research Ctr., Cambridge, Mass., Tech. Rpt. No. AFCRC-TR-102; July, 1954

[9] G. C. Southworth, "Principles and Applications of Waveguide Transmission," D. Van Nostrand Company, Inc., New York, N. Y., Sec. 10.1, pp. 402–411; 1950.

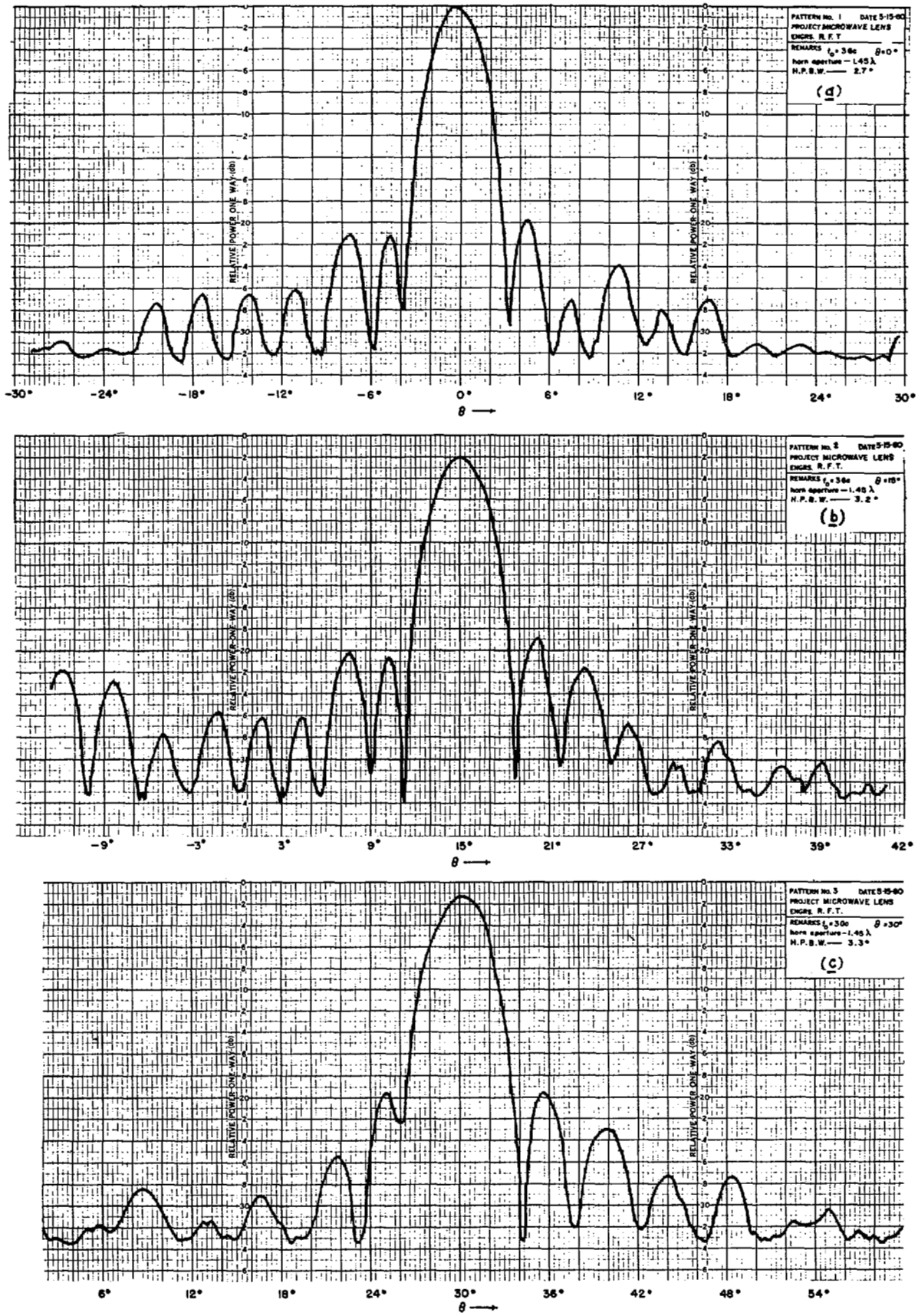

Fig. 6—Radiation patterns of microwave lens antenna. (a) $\theta=0°$ (on-axis). (b) $\theta=15°$. (c) $\theta=30°$.

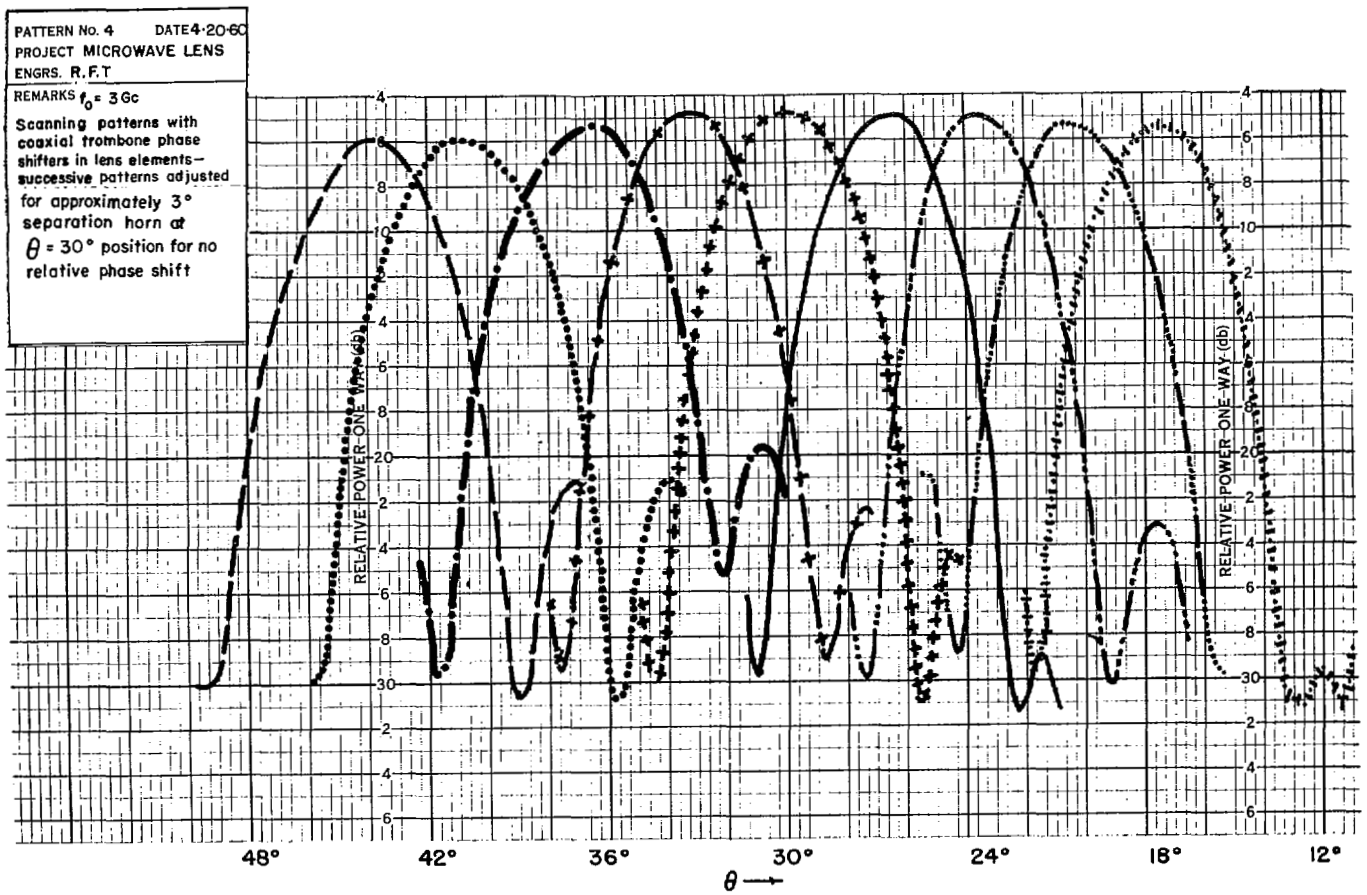

Fig. 7—Radiation patterns of lens antenna with phase shifters in lens elements.

Radiation patterns of this lens model were measured for a variety of input horns, focusing positions and operating frequencies from 2.8 to 3.2 Gc. Representative patterns are shown in Fig. 6 for a frequency of 3 Gc. The position of best focus for the input horn was not critical and almost on the focal arc in all cases. The measured sidelobe levels of −18 db, which were poorer than the −22 db design value, were probably caused by a nonoptimum horn aperture which would also account for a measured beamwidth smaller than the theoretical value.

The antenna beam of the wide-angle microwave lens can also be scanned by adding linearly progressive, variable phase delays in the coaxial lens elements which cause a relative phase shift between successive probe radiators and a corresponding angular change in the position of the radiation pattern. Coaxial phase shifters were therefore added to all the lens elements in the model to provide a beam-scanning capability. Although each of the stationary input horns generated a beam which points in a different direction, all the beams can be moved simultaneously by varying the phase shifters with a phase increase which is proportional to their distance along the aperture. The entire field of view of the lens may be covered by several independent beams, each of which scans only a small sector, if the spacing of the input horns are properly chosen. Although the development of this antenna concept, the Multiple-Beam Interval Scanner (MUBIS) system, was not completed due to its supercession by an antenna system[10,11] which used the wide-angle microwave lens and coaxial organ-pipe scanners, a study was made of the application of these coaxial phase shifters of the trombone or line stretcher type to beam scanning. The phase shifters were adjusted to increase the cable lengths linearly along the lens face. Radiation patterns are shown in Fig. 7 for the case in which the input horn is located at 30° and where the line stretchers are adjusted to scan the beam ±12° about this central value in 3° steps. It can be seen that the gain of the antenna and the pattern shape do not change appreciably even for these large scan angles (42° maximum). Similar patterns have been obtained where the input horns were placed at 0° and 15°.

[10] L. Blaisdell, "Multiple beam interval scanner antenna system," Sylvania Electronics System Lab., Waltham, Mass., Interim Engrg. Rept., Contract No. AF19(604)-7385; November, 1960.

[11] W. Rotman and F. LaRussa, "An electro-mechanically scanned lens antenna for space surveillance," Northeast Electronics Research and Engineering Meeting, Record, pp. 100–101; November, 1962.

Conclusions

The design principles presented for two-dimensional lenses may also be applied with advantage to three-dimensional structures since the extra degree of freedom, obtained in the Gent design by nonuniform lens element spacing, can be used to minimize phase errors over the face of the lens. It can be shown[12] that a three-dimensional, wide-angle, axially symmetrical lens is not attainable if the Ruze constraints are applied. This restriction is removed by the Gent design since the inner contour of this lens is determined, not only by the required scan angle α (as in the Ruze design), but also by the on-axis focal position g which can be specified arbitrarily. Thus, a three-dimensional lens with one planar face and with minimum astigmatism may possibly be designed as a figure of revolution of the two-dimensional lens for which the g parameter is chosen appropriately.

As an alternate suggestion, the basic Gent lens equation may contain a solution for the design of an axially symmetrical three-dimensional lens with a perfect off-axis focus when both lens surfaces may be nonplanar. Since these lens studies are beyond the scope of the present investigation, this possibility has not been further explored.

Our analysis has shown that microwave lenses with straight front faces can scan wide-angle sectors with fractional-degree beamwidths. Design and constructional techniques have been developed for use of these line sources as primary feeds for cylindrical reflectors or in planar arrays where very large antenna gains are required.

[12] "Investigation of variable index of refraction lenses," Sperry Gyroscope Company, Great Neck, N. Y., Sperry Final Engrg. Rept. No. 5224-1263, Signal Corps Contract No. DA36-039-sc-15323; September, 1952.

Appendix

Lens Contour Calculations

A short table of the variables x, y and w vs η has been computed for the straight-front-face lens design from (8), (11) and (12) and are listed for the following parameters: $\alpha=30°$, $g=1.137$, $\eta=0<0.05>0.80$ and $r=R/F=0.597$. The value of g has been selected to optimize the lens design for the given scan angle α. This lens contour is shown graphically in Fig. 3(c).

For more extensive tables for other values of g and for smaller increments of η, see Rotman and Turner.[5]

η	w	$-x$	y
0.00	0.00000	0.00000	0.00000
0.05	0.00011	0.00121	0.04999
0.10	0.00042	0.00483	0.09996
0.15	0.00091	0.01084	0.14986
0.20	0.00153	0.01922	0.19969
0.25	0.00217	0.02993	0.24946
0.30	0.00273	0.04290	0.29918
0.35	0.00301	0.05803	0.34895
0.40	0.00273	0.07519	0.39891
0.45	0.00147	0.09416	0.44934
0.50	−0.00142	0.11461	0.50071
0.55	−0.00701	0.13600	0.55385
0.60	−0.01717	0.15739	0.61030
0.65	−0.03543	0.17699	0.67303
0.50	−0.06935	0.19097	0.74855
0.75	−0.13861	0.18940	0.85395
0.80	−0.3172	0.1349	1.054